Quantification of parallax errors in sky simulator domes for clear sky conditions

J Mardaljevic

Lighting Research and Technology 2002 34: 313
DOI: 10.1191/1365782802li055oa

Lighting Res. Technol. 34,4 (2002) pp. 313–332

Quantification of parallax errors in sky simulator domes for clear sky conditions

J Mardaljevic BSc MPhil PhD
Institute of Energy and Sustainable Development (IESD), De Montfort University, Netherleys Building, Scraptoft, Leicester LE7 9SU, UK

Received 27 March 2002; accepted 14 June 2002

Scale model illuminance measurements in sky simulator domes are inherently subject to parallax errors. The magnitude of these errors under a number of Commission Internationale de l'Éclairage (CIE) clear sky configurations is quantified using computer simulation techniques. In practical operation of a sky simulator dome, a second parallax error in the normalization measurements for horizontal illuminance is likely to compound the parallax error in the other illuminance measurements. This additional parallax error is accounted for in the simulations. The concept of a parallax-bounded volume is introduced. This is the volume of the dome which, on the basis of parallax alone, must contain a scale model if it is not to be subject to errors in the measurement of illuminance beyond a given tolerance. The findings indicate that, on the basis of a credible design goal for the sky simulator dome, high accuracy illuminance predictions (±10%) are practically unattainable.

1. Introduction

Daylight modelling under non-overcast sky conditions has received considerable attention in recent years. Various theoretical formulations of non-overcast sky luminance distributions have appeared in the literature since the mid-1970s. Worldwide studies such as the International Daylight Measurement Programme (IDMP) have produced a vast body of empirical data on daylighting parameters. These range from extensive monitoring of basic daylight quantities to long-term measurements of the sky luminance distribution. The sky luminance distribution data have been used to test the performance of a number of sky models.[1,2] Simultaneous measurements of sky luminance distributions and internal daylight illuminances have been used to test computer predictions of internal illuminances under real sky conditions.[3–5] Furthermore, the efficient prediction of hourly internal illuminance levels for a full year has been demonstrated using lighting simulation techniques.[6–8] For physical modelling approaches, there are now two artificial sky simulator domes (SSDs) in the UK that are capable, in principle, of modelling any sky luminance distribution.[9,10] The dome at University College London (UCL, UK) is 5.4 m in diameter and has 270 lamps to provide sky illumination. The dome at the Welsh School of Architecture (Cardiff University, UWCC) is larger, 8 m in diameter and has 640 lamps. Similar examples further afield include the scanning sky simulator at the EPFL in Lausanne (Switzerland),[11] the Bartenbach LichtLabor (Austria) dome (diameter 6.5 m, 393 lamps)[12] and the Sekisui Corporation's all-sky simulator in Nara (Japan). The Sekisui sky simulator is reputed to have cost one million $US.[13] Evidently, the modelling of

Address for correspondence: J. Mardaljevic, Institute of Energy and Sustainable Development, De Montfort University, Netherleys Building, Scraptoft, Leicester LE7 9SU, UK. E-mail: Jm@dmu.ac.uk

10.1191/1365782802li055oa

daylight under non-overcast skies is an area of considerable research activity, underpinned by significant capital investment in the construction of several sky simulator domes.

It has long been appreciated that scale modelling in artificial skies under non-uniform luminance distributions is prone to parallax errors. These arise because the effective luminance distribution 'seen' at a point varies depending on the position of the point. This is so for any non-uniform luminance distribution including, of course, the Commission Internationale de l'Éclairage (CIE) Standard Overcast Sky where the zenith luminance is three times that of the horizon. A recent paper by Lynes and Gilding[14] described an investigation into parallax errors for the CIE Standard Overcast Sky. The authors note that:

> The parallax error could well be exacerbated if the overcast distribution is replaced by, say, a clear sky or an 'average' sky characterised by gradients of luminance.

The work of Lynes and Gilding is expanded upon in this paper to quantify the effect of parallax errors for non-overcast luminance distributions – precisely the conditions that the new sky simulators are intended to model.

2. Parallax in SSDs

SSDs that reproduce non-uniform luminance patterns are inherently subject to parallax errors because the angular distribution of luminance is 'correct' only for the centre point, i.e., $L_a \neq L_o \neq L_b$ (Figure 1). Any point away from the centre will 'see' a luminance pattern that is different from the 'correct' distribution, in other words: a parallax error. The change in luminance distribution that can result from parallax errors is illustrated in Figure 2. The images show the view of a CIE clear sky luminance pattern mapped onto a dome of finite size as seen from three different points along the north–south diameter. The CIE clear sky luminance pattern was generated for a sun position that was due south at altitude 45°, this is marked M on the accompanying diagrams. The view for each case was horizontal, level with the horizon and directed due south. The first image (a) shows the 'correct' (or zero-parallax) view of the luminance distribution as seen from the origin. Image (b) shows the luminance distribution that is visible from a point mid-way to the north 'horizon' (i.e. edge of the dome). The peak in luminance distribution is now at a lower altitude and sky that lies to the north of the zenith is now seen at the edges of the hemispherical field of view. The view point in the last image (c) is now mid-way towards the horizon in the south, and the peak in the luminance distribution is seen at a higher altitude than the correct value of 45°. Illuminance is the integral of luminance over the projected (i.e. cosine-weighted) hemisphere. Thus for any point not at the origin, the change in the 'visible' luminance distribution will result in deviation of the received illuminance from the correct (i.e. zero-parallax) value at the origin. Evidently, parallax errors will be present when illuminances are measured at any point in a sky simulator other than the origin, for non-uniform luminance distributions. The questions addressed here are: how large are these errors likely to be and how can they be quantified in a systematic way.

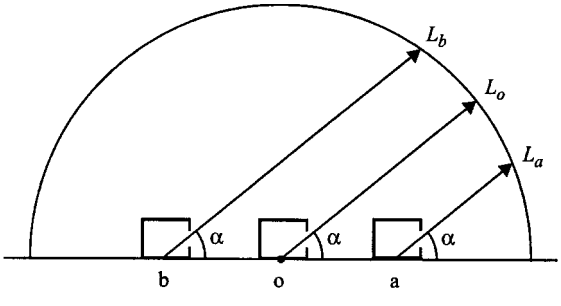

Figure 1 Parallax errors in SSDs

2.1 Design goal for SSDs

SSDs are intended to reproduce a wide range of sky luminance patterns, from overcast through to clear skies with the possibility perhaps of including real sky luminance patterns measured by sky scanners. It is not practicable to evaluate parallax errors in SSDs for all sky types, since

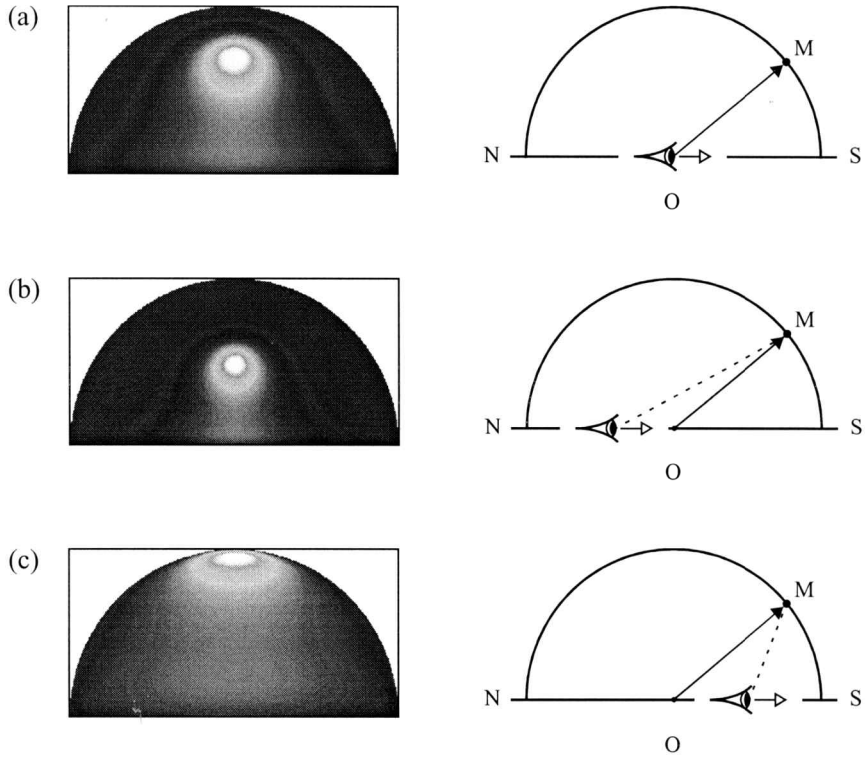

Figure 2 Hemispherical fish-eye views of the CIE clear sky distribution looking south from (a) the origin, i.e., zero-parallax, (b) mid-way to the north horizon and (c) mid-way to the south horizon

a near infinite range of sky configurations are possible. Thus a finite number of possible sky types needs to be identified. An evaluation that is too small in scope, however, may offer too limited an insight to be of practical value. A compromise between completeness and tractability was achieved by assuming the following credible, design goal for an SSD: accurate prediction of vertical south illuminance under CIE clear sky conditions for a number of possible sun positions. The rationale for this design goal was as follows. First, the vast majority of building designs have vertical glazing. If an external vertical illuminance cannot be accurately predicted, then the internal illuminances, horizontal or otherwise, will not be correct. Second, a south facing surface is exposed to a greater variation in sky luminance patterns, for a given non-overcast sky model, than other orientations. Lastly, clear sky conditions can occur for any above horizon sun position, so, ideally, the SSD should perform 'well' for any of these positions. The goal therefore is to determine, subject only to parallax errors, what volume of space within the SSD will give 'accurate' values for vertical south illuminance under a number of CIE clear sky configurations. This space is referred to here as the parallax-bounded volume or PBV. The extent of the PBV will depend on the desired accuracy, i.e., deviation from the zero parallax value. Evidently, the lower the desired accuracy, the greater the allowed parallax errors and the larger the PBV. The extent of the PBV was determined for three accuracy bands: 'high', 'medium' and 'low', which refer, respectively, to vertical south illuminances within $\pm 10\%$, $\pm 25\%$ and $\pm 50\%$ of the zero-parallax value.

The sun positions used for the evaluation of parallax error were based on the range of above-horizon sun positions that occur throughout the

year for the Midlands (UK) (Figure 3). A grid of 22 points that span a major part of the distribution were selected (+ symbols in Figure 3). These were the sun-position loci for each of the 22 CIE clear sky configurations evaluated. The points cover much of the range of possible sun positions for altitudes above 15°. The design goal therefore was an 'accurate' value of vertical south illuminance for each of the 22 CIE clear sky configurations.

Note that parallax errors due to the displacement of the sun, as 'seen' from any point in an SSD other than the origin, were not evaluated in this study. This is in part because sun parallax errors are highly sensitive to the size and photometry of the particular lamp used to model the sun. Also, the relative illuminance effect of the sun and the sky is, to a degree, arbitrary, which would greatly complicate the evaluation approach described above. Furthermore, the objective here is to evaluate the performance limit of the full sky dome rather than the heliodon, which, in terms of cost and complexity, is a lesser device than the dome, and in itself it is not a novel apparatus.

The PBV of an SSD, based on the achievement of the design goal for the three accuracy bands, was accurately determined using computer simulation techniques (see Section 2.4). Indeed, it is not a straightforward task to attempt to investigate these effects using illuminance measurements in actual SSDs because a number of confounding factors are present. Significant amongst these are incomplete sky coverage and stability of the luminous output of the lamps.[11] In contrast, with computer simulation it is possible to specify the luminous environment – geometry and sky luminance pattern – with exact precision. Furthermore, the illuminance received directly from a diffuse dome is relatively trivial to determine and can be reliably predicted with high accuracy (better than ±1%, see Section 2.4). Thus, computer simulation permits a rigorous analysis of a *fundamental* property of SSDs (i.e., parallax error) that is not contaminated by the *particular* characteristics of this or that dome (e.g., diameter, number of lamps, coverage, etc.). As such, this study delineates the theoretical limits of performance – based on the design goal – of SSDs in general. To preserve generality, only illuminance received directly from the sky dome is considered. In other words, there is no ground-reflected component of illuminance.

2.2 Determining the PBV

At present, the usable space in an SSD is not a prescribed quantity. Since it is appreciated that parallax errors will occur, keeping the model dimensions to a minimum is advised. However, it is not always easy, or even practicable, to construct building models accurately in very small scales. Furthermore, work by Cannon-Brookes[15] has shown that imprecision in model construction can be the cause of large errors when the models are used to predict illuminance. On the basis of those findings, where parallax errors were not a concern, it was recommended that building models should be made larger rather than smaller to minimize errors in construction. Thus, in SSDs where

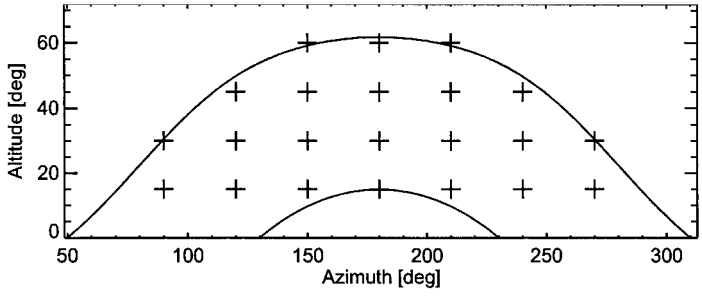

Figure 3 Sun position for the 22 CIE clear sky configurations evaluated

parallax errors are unavoidable, it is desirable to establish the maximum possible dimensions of the building model – as constrained by the PBV – that can achieve the stated design goal.

The likely extent of the PBV within the SSD was based on preliminary tests that disclosed parallax errors in excess of 50% (i.e., 'low' accuracy) for points further than $0.5R$ from the origin, where R is the radius of the dome. This scale was used to size a cuboid, or block, that encompassed the space of the SSD that was tested for parallax. The dimensions of the block were $0.9R \times 0.9R \times 0.45R$. The base was centred on the origin and the block occupies ~ 17% of the hemisphere's volume. The block was used to locate a three-dimensional array of calculation points that were equally spaced in the x, y and z directions with a separation of $0.05R$ (Figure 4). Thus the array was of size $19 \times 19 \times 10$ giving a total of 3610 calculation points. This is referred to here as the 'test volume'. The vertical south illuminance at each of these 3610 points was computed inside a dome of radius R configured to give an exact CIE clear sky luminance pattern as seen from the zero-parallax point (i.e., origin). This was repeated for each of the 22 clear sky configurations. The set of points S^T that gave a prediction within $\pm T\%$ of the zero-parallax point for all 22 clear sky configurations was determined as follows. For a particular sky configuration i, the set B_i^T is all those points p_i where the parallax error (%) in the vertical illuminance is within $\pm T\%$ of the zero-parallax point:

$$B_i^T = \{p_i : |\text{parallax error}| \leq T\} \qquad (1)$$

The PBV S^T is that collection of points that is common to all 22 B_i^T sets. In other words, a volume of intersection:

$$S^T = B_1^T \cap B_2^T \cap B_3^T \cap \ldots \cap B_{22}^T \qquad (2)$$

This is illustrated schematically in Figure 5. For clarity, only three of the B_i^T sets are shown. The renderings are visualizations of the sets B_i^T where the vertical south illuminance is within $\pm T\%$ of the zero-parallax value. For this illustration, the white marker shows the point in space where the evaluation was made. In order to visualize the volume delineated by the points, a cube of side equal to the spacing between the points was placed 'behind' each one. Thus the points are on the south-facing side of the cubes. The light- and dark-shaded cubes indicate over-prediction and under-prediction, respectively (for points within the given error band). This is of course an example of a Venn diagram showing the region (here, volume) of intersection of a number of sets. To recap, the set of points S^T describes the PBV of the SSD for prediction of vertical south illuminance within the given error band $\pm T\%$ for all 22 CIE clear sky configurations. In practice, more than one type of parallax error may

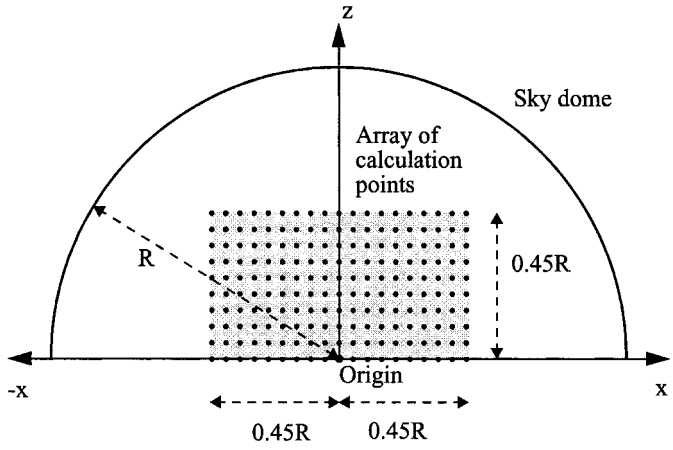

Figure 4 Volume of dome assessed for parallax errors

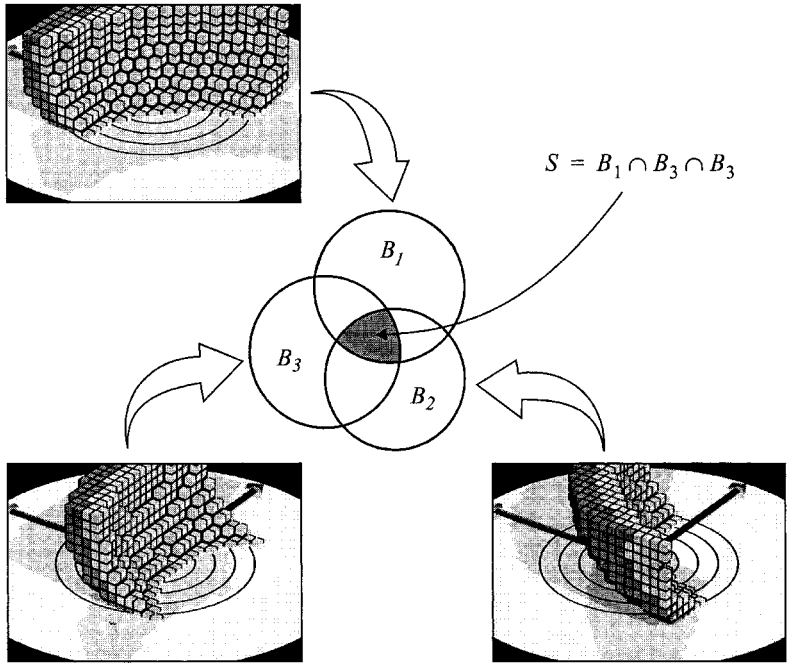

Figure 5 Schematic illustrating the intersection of volumes containing points within a given error band (only three of the 22 are shown)

occur in an SSD; they are described in the following section.

2.3 Simple and compound parallax errors

At first sight, it may seem that the parallax error in vertical illuminance is simply due to the difference between the vertical illuminance V_o at the origin and the vertical illuminance V_p measured elsewhere. This difference is referred to here as the simple parallax error S_{PE}. Expressed as a percentage it is:

$$S_{\mathrm{PE}} = \left(\frac{V_p - V_o}{V_o} \right) \times 100\% \qquad (3)$$

However, an additional error, also resulting from parallax, is likely to be introduced because of the way SSDs are operated in practice.

It is generally the case that illuminance measurements for a scale model need to be normalized using a simultaneous measurement of unobstructed horizontal illuminance. In part, this is because SSDs cannot reproduce the very high absolute illuminance levels that occur on bright days. In principle, this should not be a drawback because, provided the luminance distribution is correct, the measured illuminances can be scaled (i.e., normalized) to arbitrary large absolute levels as desired. In the usual mode of operation of an SSD, the lamps are programmed to reproduce a particular luminance distribution (e.g., CIE clear sky) – no attempt is made to achieve a specific horizontal illuminance level. It is understood that factors relating to the control and functioning of the luminaries (e.g., the range and stability of the luminous output) necessitate this approach. Thus, for each sky modelled in an SSD, the horizontal illuminance that it produces is not known *a priori* and must be measured. This measurement is referred to here as the normalization illuminance. The usual practice is that the normalization illuminance (i.e., unobstructed horizontal illuminance) is taken simultaneously with each one or more illuminance measurements for the scale model. The most practical

way to achieve this is to place a photocell on top of the scale model (Peter Raynham, UCL, 15 January 2001, private communication). Once the normalization illuminance is known, the other illuminance measurements can be scaled to be in accord with any desired absolute value for horizontal illuminance, called here the 'set-point'. For the scenario used in this analysis, it would mean that the horizontal illuminance is measured at the same time as the vertical south illuminance. If measured anywhere other than the origin, which is likely to be the case when a scale model is present, the horizontal illuminance will be subject to its own parallax error. This will add to the already present (i.e., simple) parallax error in the vertical illuminance giving what is referred to here as the compound parallax error, or C_{PE}.

C_{PE} is determined as follows. The diffuse horizontal set-point H_d can be any value and it is used to convert illuminance measurements in SSDs to 'real-world' illuminances. For example, say that the SSD was programmed to reproduce clear sky conditions and that the (unobscured) horizontal illuminance at the zero-parallax point (i.e., origin) was measured to be H_o. Other measurements taken in the SSD can then be scaled to the set-point horizontal illuminance by multiplying them by the normalization factor H_d/H_o. However, if the normalization illuminance is measured at n instead of the origin, the normalization factor used will be H_d/H_n, which contains a parallax error (Figure 6). This is factored into the measurement of other illuminances when they are normalized to the set-point H_d. C_{PE} is calculated using the vertical illuminance V_p normalized using H_d/H_n, and the zero-parallax vertical illuminance V_o normalized using the zero-parallax factor H_d/H_o. C_{PE} is therefore:

$$C_{\mathrm{PE}} = \left(\frac{V_p\left(\frac{H_d}{H_n}\right) - V_o\left(\frac{H_d}{H_o}\right)}{V_o\left(\frac{H_d}{H_o}\right)} \right) \times 100\% \quad (4)$$

Since the set-point illuminance is arbitrary, Equation 4 can be simplified by using $H_d = H_o$ to give:

$$C_{\mathrm{PE}} = \left(\frac{(V_p H_d/H_n) - V_o}{V_o} \right) \times 100\% \quad (5)$$

In principle, the normalization illuminance can be measured at any point on or around a scale model in an SSD that gives the least obstructed view of the sky dome. In practice, it is likely to be the case that the SSD users will attempt to minimize the parallax errors by placing the normalization photocell on top of the scale model and directly above the origin, in other words, along the z-axis.

As the compound parallax error involves two illuminance values, V_p and H_n, that are measured at different points, p and n, the magnitude of the C_{PE} will be sensitive to the relative location of the points. The effect of the relative positioning of the normalization photocell to the vertical illuminance photocell was determined for two locating strategies. In the first, the normalization illuminance was evaluated at the height of the vertical illuminance photocell p_z plus $0.05R$ (Figure 7b). Here the normalization photocell is at the minimum possible height above the vertical illuminance photocell (for the grid spacing used in this analysis). For the second locating strategy, the normalization illuminance was evaluated at a height equal to twice that of the vertical illuminance photocell, i.e., 2 p_z (Figure 7a), except for when $p_z = 0$, where the first strategy is used. Recall that the z-dimension of the block extends from $z = 0$ to $z = 0.45R$. So, to provide normalization illuminances for both locating strategies, the normalization illuminance was evaluated at points along the z-axis from the origin (i.e., the zero-parallax value) to $z = 0.9R$ in steps of $0.05R$. The locating strategies are summarized as follows:

$$\text{Locating strategy 1: } n_z = p_z + 0.05R \quad (6)$$

$$\text{Locating strategy 2: } n_z = p_z + 0.05R \quad \text{for } p_z = 0$$
$$n_z = 2p_z \quad \text{for } p_z > 0 \quad (7)$$

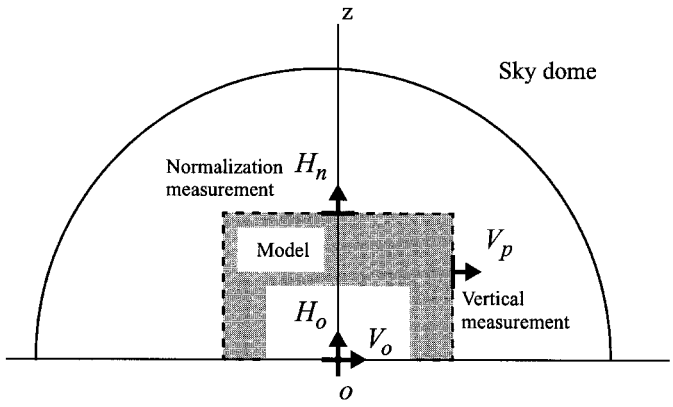

Figure 6 Schematic showing relative position of calculation points for vertical illuminance and normalization

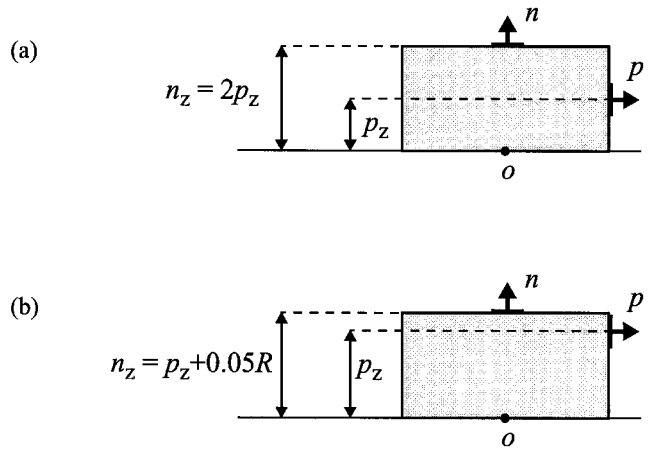

Figure 7 Locating strategies for the relative position of the vertical and horizontal illuminance evaluation points

When evaluated on top of the building model, the normalization photocell has an unobstructed 'view' of the sky dome, though, as noted earlier, at any height above the origin there is a parallax error because the photocell doesn't 'see' the full hemisphere of the sky. Parallax error notwithstanding, when the view is unobstructed, the horizontal illuminance received at the photocell is invariant to rotation of the sky (or model) about the z-axis. Thus, the normalization illuminance needed to be evaluated only for those CIE clear sky configurations with unique sun altitudes, i.e., 15°, 30°, 45° and 60° (Figure 3).

2.4 Computation of parallax errors

The effect of parallax errors on illuminance modelling in SSDs was quantified using computer simulation. The rigorously validated *Radiance* lighting simulation system[16] was used to predict vertical and horizontal illuminance quantities in an SSD of unit radius ($R = 1$) for a range of CIE clear sky configurations (Figure 3). The SSD was modelled as a diffuse emitting hemisphere. The CIE clear sky luminance distribution was mapped onto the dome as a continuous pattern in exact accordance with the standard equation.[17] The CIE clear sky model is nor-

malized to zenith luminance L_ζ, and the luminance L_q of the sky at point q on the sky vault is given by:

$$L_q = L_\zeta \frac{(0.91 + 10e^{-3\theta} + 0.45\cos^2\theta)\,(1 - e^{(-0.32/\sin\gamma)})}{(0.91 + 10e^{-3(\pi/2-\gamma_s)} + 0.45\sin^2\gamma_s)\,(1 - e^{-0.32})} \quad (8)$$

where γ_s is the zenith sun angle, θ is the angle between the sun and q, and γ is the zenith angle of q.

As noted, illuminance is the integral of luminance over the projected hemisphere. The *Radiance* system was used to solve the luminance integral using hemispherical sampling. The number of ray samples for each computation was set to 4096 (though the actual number used will vary slightly from this value). This number of ray samples was determined from tests carried out to ensure that sufficient rays were used each time to guarantee accurate predictions, i.e., within 1% of a fully converged result. Interpolation was disabled to ensure that ray sampling was initiated from every calculation point. These procedures effectively eliminate any significant source of error in the *Radiance* predictions – they can be taken as accurate to better than 1% and more than adequate for the quantification of parallax errors. The vertical south illuminance was computed at each of the 3610 calculation points (Figure 4) for the 22 different clear sky configurations (Figure 3), giving a total of 79 420 computations. The horizontal illuminance used for normalization was predicted at 19 points along the z-axis for each of the four unique sun altitudes giving a total of 76 computations. The results are described in the next section.

It should be noted that parallax errors are entirely avoided in the normal use of the *Radiance* program by modelling the sun and sky as source solid angles.[16] In this way the sky and sun are effectively infinitely distant from the local scene. Hence the luminance pattern on the sky vault is invariant to position in the local scene and parallax errors do not occur.

3. Results

The magnitude in the simple parallax errors for vertical and horizontal illuminance that can occur in an SSD are shown in Figures 8, 9 and 10. The first two plots show the parallax error in vertical illuminance across the north–south diameter (Figure 8) and the positive z-axis (Figure 9). The parallax error in horizontal illuminance along the positive z-axis (i.e., the normalization illuminance) is given in Figure 10. In each case, curves are given for CIE clear sky configurations with the sun due south at altitudes 15°, 30°, 45° and 60°. The linear extent of the test volume (bold line with bars) is shown on each plot. Most striking is the sensitivity of the parallax error in vertical south illuminance along the north–south diameter for the various sun altitudes (Figure 8). As expected, close proximity to the circumsolar region of the luminance pattern (i.e., towards the south) results in illuminances higher than the zero-parallax value of 100 lux. Conversely, illuminances to the north of the origin are lower than the zero-parallax value, but the effect is less pronounced. The variation in vertical south illuminance along the z-axis (Figure 9) shows consistent over-prediction towards a peak value for each curve, followed by reduction of the error and a change of sign for two of the lines. Recall that horizontal illuminance evaluated along the z-axis is used to calculate C_{PE} (Section 2.3). How this quantity alone varies with height is shown in Figure 10. Here the effect of parallax is to give lower illuminances than the zero-parallax value for all sun altitudes except at 60°. The line plots are instructive, but it is not possible to infer from these how the *space* within the SSD is affected by parallax errors, simple or compound. How this was accomplished is described in the following section.

The PBVs are presented as visualizations of the set of points S^T for the various error types, accuracy bands and locating strategies. The PBVs for the simple parallax error are shown in Figure 11. Note, as well as computing the luminance integrals to predict illuminance, the *Radi-*

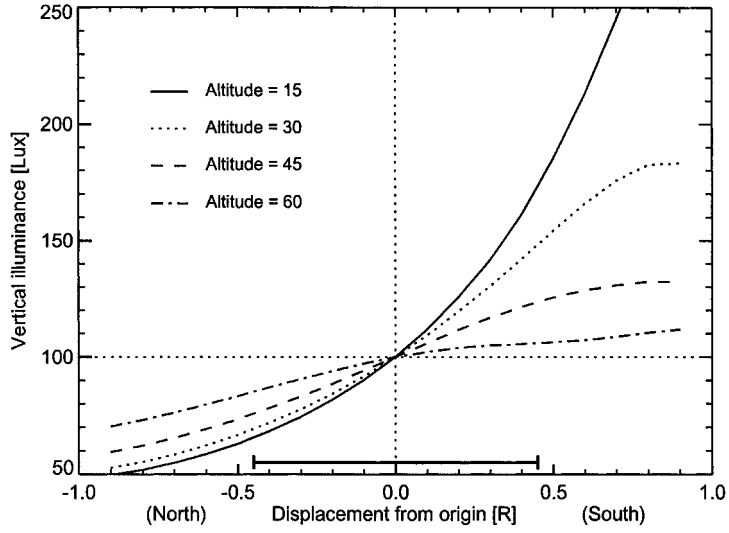

Figure 8 Parallax error in unobstructed diffuse vertical south illuminance along the north–south diameter of an SSD under CIE clear sky conditions at solar noon

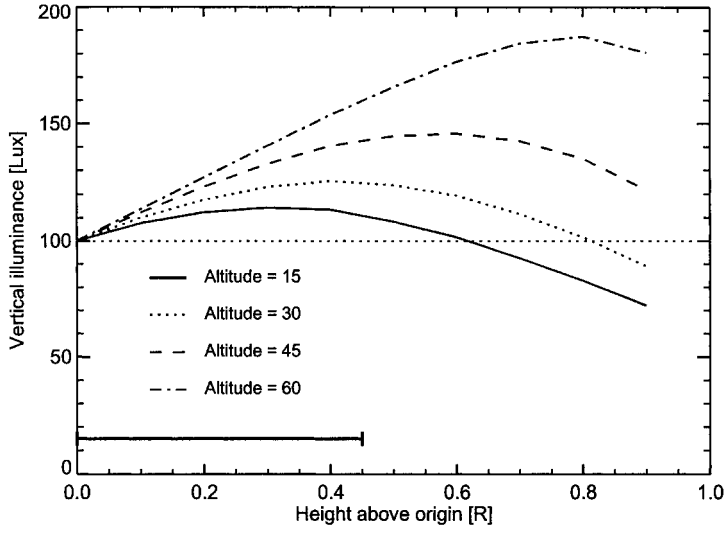

Figure 9 Parallax error in unobstructed diffuse vertical south illuminance along the *z*-axis of an SSD under CIE clear sky conditions at solar noon

ance program was also used to generate the visualizations (i.e., renderings) of the PBVs. The markers co-incident with the ring (i.e., ground) plane show those positions where an 'accurate' prediction was achieved for a point in the plane of the base of the dome. In other words, at height zero. For practical scale modelling, these points are unlikely to be usable unless the physical model could be positioned below the ground plane (a plausible arrangement perhaps for the evaluation of designs with roof lights). The renderings in Figure 11 show that the extent of the PBV is very sensitive to the accuracy band. For low-accuracy predictions of vertical south illum-

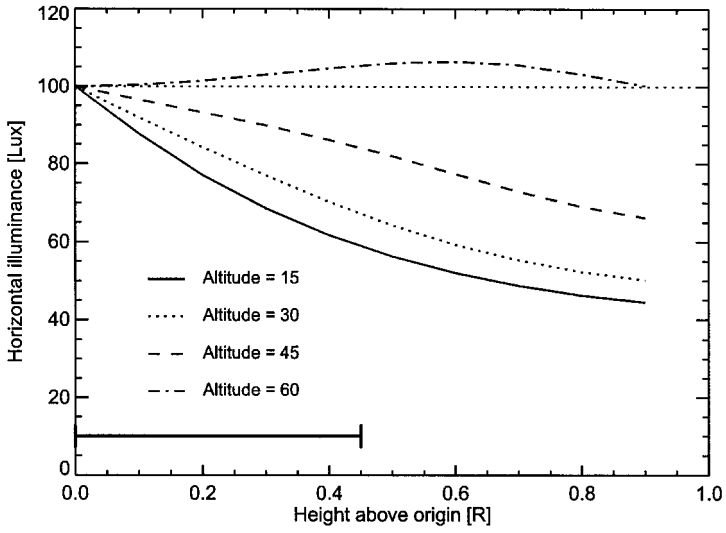

Figure 10 Parallax error in unobstructed diffuse horizontal illuminance along the *z*-axis of an SSD under CIE clear sky conditions at solar noon

inance (i.e., within ±50% of the zero-parallax value), the PBV clearly extends beyond the region of space tested. For medium-accuracy (±25%) predictions, the PBV is markedly smaller with a north–south dimension of ~ 0.5*R* and a height of ~ 0.2*R*. At high accuracy, there are only three points above the ground plane where the vertical south illuminance is within ±10% of the zero-parallax value. This PBV could just contain a building model that is ~ 0.15*R* long, ~ 0.05*R* wide and ~ 0.05*R* high. Applying these scales to the UWCC sky simulator dome (4 m radius), the building model would have dimensions ~ 60 × ~ 20 × ~ 20 cm. Applied to the UCL dome (2.7 m radius), the dimensions would be ~ 40 × ~ 14 × ~ 14 cm.

In standard operation of an SSD, it is expected that normalization of the vertical illuminance measurements will introduce a second type of parallax error called the C_{PE} (Section 2.3). Including this factor in the calculation of the parallax error (Equation 5) results in a diminution of the PBV for all three accuracy bands (Figure 12). The principal effect of including the normalization error is to significantly reduce the height of the PBV, this is readily apparent in the renderings. As expected, this effect is greatest with the second locating strategy. Notice that for $p_z = 0$ and $p_z = 0.05R$ the locating strategies (Equations 6 and 7) give the same values for n_z. Accordingly, the pattern of box-markers at these two heights is the same for both. Most striking is the observation that high-accuracy predictions (±10%) of vertical south illuminance were not achieved for any points above the ground plane. In fact, for high-accuracy predictions, both locating strategies produced the same PBV: nine points level with the ground plane (accordingly, only one rendering of the PBV is shown).

The results for both simple and compound parallax errors are given in tabular form also (Table 1). It is possible to relate the maximum dimensions of a scale model – as constrained by the PBV – to the diameter of an actual SSD by approximating the PBV to the shape of a cube. The volume associated with each point of the set S^T is $(0.05R)^3$, and for the N points above the ground plane, the total volume is $N\ (0.05R)^3$. This volume is equivalent to a cube of side D where:

$$D = 0.05R(N^{1/3}) \qquad (9)$$

This relation is plotted in Figure 13 for the medium and low accuracy bands using both

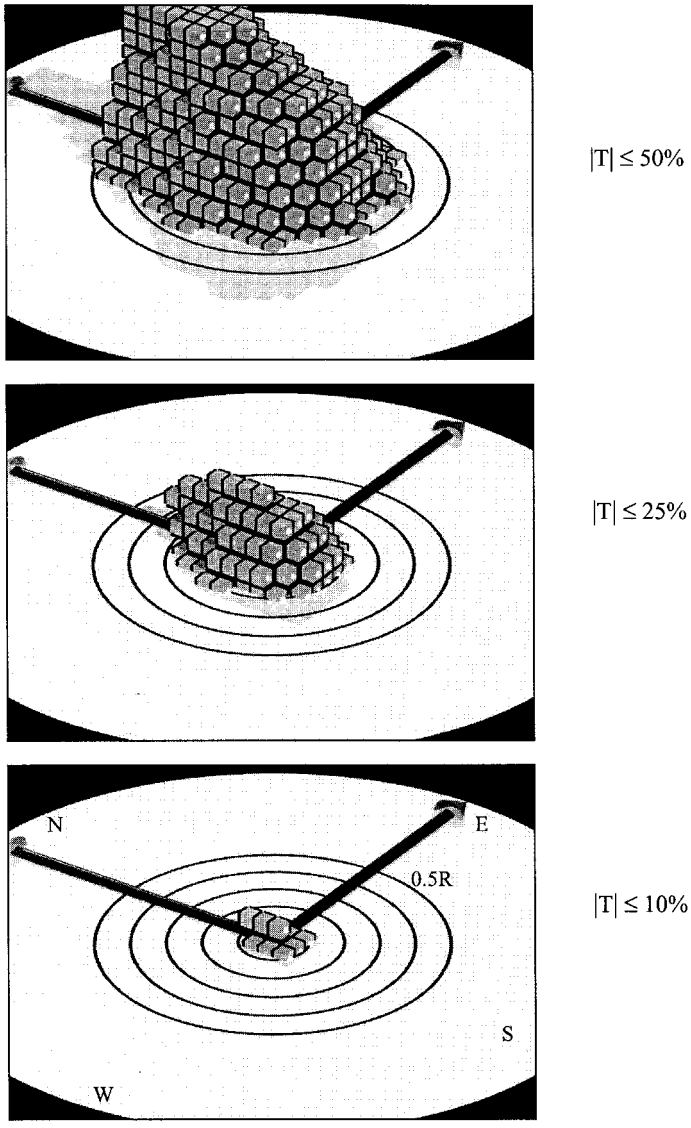

Figure 11 Results for simple parallax error

locating strategies. The diameter of the SSDs at UCL and UWCC are marked. It is clear from the renderings of the PBVs that a cube is a crude approximation to their actual shape. In actual use, to be enclosed by the PBV, a scale-model would have a depth and width greater than D, and a height less than D.

4. Discussion

The PBVs for SSDs under clear sky conditions have been evaluated based on a credible design goal and for a range of accuracy bands. Given the likely mode in operation of an SSD, it would appear that the PBVs for C_{PE} best describe the

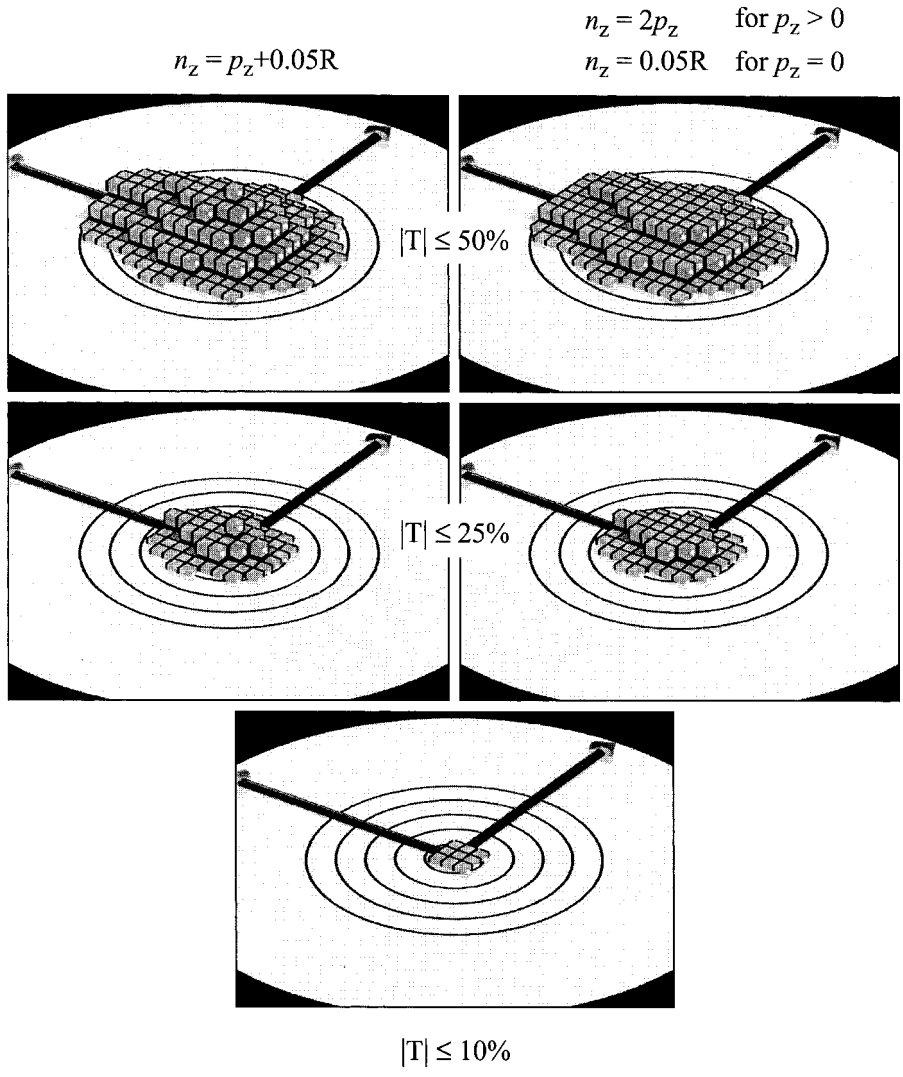

Figure 12 Results for compound parallax error

Table 1 Simple and compound parallax error results

Accuracy band	Number of calculation points within accuracy band $p_z > 0$ and ($p_z \geq 0$)		
	Simple parallax error	Compound parallax error	
		$n_z = p_z + 0.05\,R$	$n_z = 2p_z$
±50%	749 (942)	201 (394)	150 (343)
±25%	108 (171)	23 (86)	22 (85)
±10%	3 (12)	0 (9)	0 (9)

theoretical performance limit of SSDs. These findings have implications for the use and operation of SSDs and raise a number of issues:

1) High-accuracy (±10%) predictions in SSDs are practically unattainable on the basis of parallax errors alone.
2) The PBVs for medium-accuracy predictions (±25%) place quite severe limitations on scale-model dimensions, even for the 8-m dome at UWCC.
3) Any expansion of the design goal to include

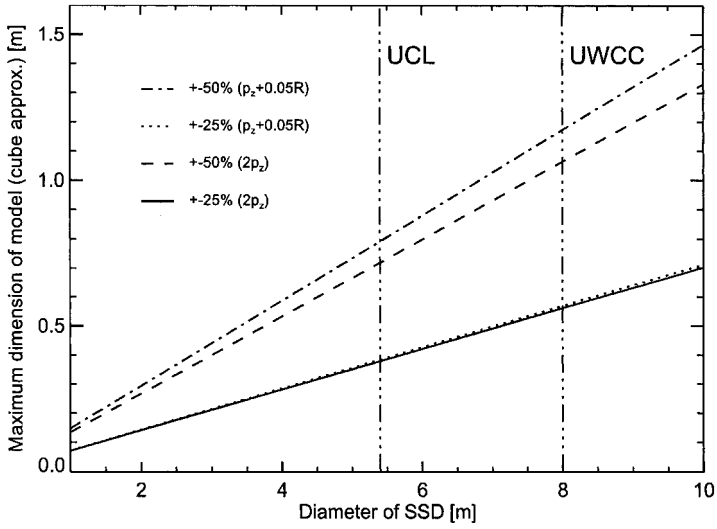

Figure 13 Maximum dimension of model versus SSD diameter (cube approximation)

a greater number of sky types and/or configurations is likely to result in further diminution of the PBV for any given combination of accuracy band and locating strategy. At best, the PBV will remain unchanged, but it cannot increase in size without relaxing the criteria for the original design goal.

4) It is expected that practical operation of an SSD will introduce a number of other factors that will add to the uncertainty of measurements taken from scale models. For example, less than exact reproduction of clear sky luminance patterns, incomplete sky coverage, and of course, inaccuracies in scale-model construction.
5) The sky was modelled as a diffuse emitting hemisphere whereas actual SSDs are comprised of a large number of luminaires providing directional illumination. The light-field in an actual SSD therefore is likely to be more complex than that modelled here. It is difficult to anticipate how this might effect the assessment of the PBV. The parallax characteristics of a particular SSD, based on luminaire photometry, could be modelled using lighting simulation if the data were available.
6) There may be instances, say for models with low internal reflectance, where the accuracy of internal illuminance measurements is more dependent on the directly visible luminance through the window than the vertical illuminance at the plane of the window. For these special circumstances, the effective PBVs may be larger than those evaluated here. However, errors resulting from incomplete sky coverage could be quite significant when the 'view' through the window happens to include a large patch of 'black' sky between the luminaires.

This study has shown that the theoretical limits of performance of SSDs, based on parallax errors alone, are sufficient to bring into question the practicality of SSDs as an instrument for producing reliable, high-accuracy scale-model illuminance data under clear sky conditions. It would appear that no better than medium accuracy ($\pm 25\%$) is attainable, and that other confounding factors may make that difficult to achieve.

There exists a perception that physical modelling approaches give the most reliable illuminance data, and they are often used as a bench-

mark to evaluate other prediction techniques. In light of the work presented here, the earlier findings of Cannon-Brookes[15] and the already demonstrated high accuracy for computer simulation,[5] it would seem that there is considerable evidence to challenge this perception. Indeed, the accuracy of illuminance modelling in SSDs cannot be readily assumed and needs to be demonstrated.

Acknowledgements

Greg Ward (Exponent Inc., USA) provided a special version of the *Radiance* **skybright.cal** file to map the CIE clear sky luminance pattern to a dome of finite extent. A referee's comments are gratefully acknowledged.

5. References

1 Ineichen P, Molineaux B, Perez R. Sky luminance data validation: comparison of seven models with four data banks. *Solar Energy* 1994; 52: 337–46.
2 Littlefair, P. Comparison of sky luminance models. *Solar Energy* 1994; 53: 315–22.
3 Mardaljevic, J. Validation of a lighting simulation program under real sky conditions. *Lighting Res. Technol.* 1995; 27: 181–88.
4 Mardaljevic J. Validation of a lighting simulation program: a study using measured sky brightness distributions. *Proceedings of the Lux Europa 97 Conference*, Amsterdam 1997; 555–69.
5 Mardaljevic J. The BRE-IDMP dataset: a new benchmark for the validation of illuminance prediction techniques. *Lighting Res. Technol.* 2001; 33: 117–36.
6 Mardaljevic J. Simulation of annual daylighting profiles for internal illuminance. *Lighting Res. Technol.* 2000; 32: 111–18.
7 Janak M, Macdonald IA. Current state-of-the-art of integrated thermal and lighting simulation and future issues. *Building Simulation '99*, Kyoto, 1999; 1173–80.
8 Reinhart CF, Herkel S. The simulation of annual daylight illuminance distributions – a state of the art comparison of six RADIANCE based methods. *Energy Buildings* 2000; 32: 167–87.
9 http://www.cf.ac.uk/archi/research/sky.html
10 http://www.bartlett.ucl.ac.uk/sky/sky.htm
11 Michel L, Roecker C, Scartezzini J-L. Performance of a new sky scanning simulator. *Lighting Res. Technol.* 1995; 27: 197–205.
12 http://www.lichtlabor.com/
13 Muneer, T. Discussion for Michel L, Roecker C, Scartezzini J-L. Performance of a new sky scanning simulator. *Lighting Res. Technol.* 1995; 27: 197–205.
14 Lynes JA, Gilding A. Parallax in artificial sky domes, *Lighting Res. Technol.* 2000; 32: 157–60.
15 Cannon-Brookes SWA. Simple scale models for daylighting design: analysis of sources of error in illuminance prediction. *Lighting Res. Technol.* 1997; 29: 135–42.
16 Ward Larson G, Shakespeare R. *Rendering with radiance: the art and science of lighting visualization.* San Francisco: Morgan Kaufmann, 1998.
17 CIE. *Standardization of luminance distribution on clear skies*. Publication No. 22. Paris: CIE, 1973.

Discussion

Comment 1 on 'Quantification of parallax errors in sky simulator domes for clear sky conditions' by J Mardaljevic

P Raynham (Bartlett School of Architecture, University College London)

The paper by Mardeljevic represents a good way to characterize the parallax errors in dome skies. However, it represents a generalized approach to the problem. In a real Variable Luminance Artificial Sky (VLAS), the sky is made up from a number of discrete sources and is not a luminous hemisphere. This gives rise to a number of differences in the errors caused. To investigate the effect of these I have recalculated the parallax errors reported by Mardeljevic by using the Bartlett VLAS.

The Bartlett VLAS is a dome 5 m in diameter which contains 270 luminaires. Each luminaire is controlled on a digital dimmer giving 255